ISSN 0016-7932, Geomagnetism and Aeronomy, 2014, Vol. 54, No. 1, pp. 50–58. © Pleiades Publishing, Ltd., 2014.
Original Russian Text © V.G. Vorobjev, O.I. Yagodkina, 2014, published in Geomagnetizm i Aeronomiya, 2014, Vol. 54, No. 1, pp. 55–64.

Comparative Characteristics of Ion and Electron Precipitation in the Dawn and Dusk Sectors

V. G. Vorobjev and O. I. Yagodkina

Polar Geophysical Institute, Apatity Division, Kola Scientific Center, Russian Academy of Sciences, Academgorodok, 26a, Apatity, Murmansk region, 184209 Russia

e-mail: vorobjev@pgia.ru

Received April 22, 2013

Abstract—Characteristics of ion and electron precipitations in the dawn and dusk sectors are investigated by DMSP F6 and F7 satellite observations. It is shown that in the dusk sector the positions of electron and ion precipitation boundaries are nearly coincident for all levels of magnetic activity; however the latitudinal distribution of energy fluxes indicates that the positions of electron and ion precipitation maxima are spatially separated. Maximum energy fluxes of ions is observed at the equatorial precipitation boundary, while those of electrons at the poleward one. In the dawn sector, the electron precipitation region is 3°–4° wider than that of ions. The isotropy boundary in the dusk sector is located in the region of diffuse precipitation (DAZ) near its poleward boundary for all levels of magnetic activity, while in the dawn sector it falls in the region of structured precipitations (AOP). Electron precipitations are dominating in the dawn sector. Here in the region of diffuse precipitation (DAZ), the ion energy fluxes Fi make less than 5% as compared to the electron energy flux Fe. In the region of structured precipitations (AOP), the portion of Fi decreases with increasing magnetic activity from ~10–20% for $AL \approx -100$ nT to <5% for $AL \approx -1000$ nT. As for the dusk sector, in the AOP region, electron precipitations are dominating as well, while in the DAZ region the ion energy fluxes are significant. In the 1500–1800 MLT sector, the ratio Fi/Fe increases from ~0.7 to ~3.0 with AL changing from –100 nT to –1000 nT.

DOI: 10.1134/S0016793214010162

1. INTRODUCTION

Many researchers have estimated the ion precipitation characteristics and the proton contribution to the total auroral precipitation pattern. Vegard (1939) first of all detected hydrogen emissions, which are an indicator of proton precipitation, using ground-based optical observations. When Meinel (1951) studied the Doppler Hα emission shift, he indicated that protons precipitate in the auroral zone. These observations allowed him to conclude that proton precipitation is observed within the ring zone and spatially coincides with electron precipitation. The characteristics of ion precipitation were subsequently studied using ground-based and satellite observations. Based on optical observations and satellite measurements of precipitating particles, it was concluded (Akasofu, 1974; Feldstein and Galperin, 1985; Gussenhoven et al., 1987) that a diffuse ion precipitation zone exists equatorward of the discrete auroral oval during the dusk and premidnight hours. Based on incoherent scatter radar data and satellite observations of precipitating particles, Basu et al. (1987) and Senior et al. (1987) concluded that protons are the main source of ionization in this region.

An extensive review of auroral proton observations was performed in (Evlashin, 2000). The main conclusions of this review were reduced to the fact that hydrogen emissions are present in green diffuse auroras, but not every diffuse aurora emits hydrogen emissions. For example, pulsating diffuse auroras in the dawn sector do not include hydrogen emissions. It was noted that hydrogen emissions move equatorward with increasing MLT in the dusk sector and poleward after midnight; protons precipitate equatorward of bright rayed auroras in the dusk sector, whereas the pattern is inverse in the dawn sector.

Reidler (1972) and Reidler and Borg (1972) tried to create a global ion precipitation model based on the ESRO satellite data. However, the statistical data set and the spectral interval of measurements on the ESRO satellite were limited during these studies. Taking into consideration the method proposed in these works, Hardy et al. (1989) developed the first statistically justified model of ion precipitation, using the DMSP F6 and F7 satellite observations. The 3-h *Kp* index was used as a geomagnetic activity parameter. These authors indicated that the region where the ion energy distribution is maximal is C-shaped and has the average energy maximum on the dusk near the ion precipitation equatorward boundary, which shifts toward noon with increasing magnetic activity. It was concluded that the proton oval in the dusk sector is statistically located equatorward of the electron oval determined by Hardy et al. (1985).

Studying the morphology and dynamics of the auroral proton luminosity, Immel et al. (2002) and Burch et al. (2002) detected subauroral proton arcs in the postnoon–dusk sector. Similar phenomena were also found by Bisikalo et al. (2003) based on the IMAGE satellite observations of proton auroras. The proton energy flux in such auroras was 0.5–2.0 erg cm^{-2} s^{-1}, and the precipitating proton energy was 10–17 keV. Based on studying proton precipitation during quiet periods and substorms, Coumans et al. (2002) indicated that the contribution of proton precipitation is larger under quiet conditions than under disturbed ones. An analysis of the IMAGE data in the N_2 LBH, NI, and Lyman-α emissions confirmed the previously achieved result that the proton precipitation oval is shifted equatorward relative to electron precipitation in the dusk sector (Coumans et al., 2002).

The brief review presented above indicated that ions can substantially contribute to the dusk sector precipitation only. This causes a certain asymmetry on the dawn–dusk meridian, which, as well as the electron–ion precipitation flux characteristics during this geomagnetic local time, have not been studied in detail. Therefore, the main aim of this work is to study the comparative characteristics of the electron and ion precipitation in the dawn and dusk sectors depending on the geomagnetic activity level.

2. USED DATA

To study the precipitation characteristics, we used the database for 1986, created previously based on the DMSP F6 and F7 satellite observations (Vorobjev and Yagodkina, 2005). The database includes more than 35000 satellite crossings of the auroral precipitation region in all MLT sectors. The satellite data were taken from the JHU/APL webpages (http://sd-www.jhuapl.edu/). The satellite detectors measured electron and ion fluxes in 20 energy channels at energies varying from 32 eV to 30 keV. For each satellite pass, the database includes information regarding the boundaries of different precipitation types, average electron and ion characteristics in these regions, geomagnetic activity level, interplanetary medium state, and the substorm phase. When we processed the data in order to increase the statistical significance of the results, we combined all passes in 3-h MLT intervals. As a measure of magnetic activity, we used the *Dst* and *AL* indices, which give rather complete information on the intensity of the geophysical processes proceeding in the Earth's magnetosphere and ionosphere. Since the satellites cross the precipitation region during 3–5 min, we used 5-min *AL* index values. We previously studied the electron precipitation characteristics using this scheme, as a result of which we created an auroral precipitation model and placed it on the website http://apm.pgia.ru (APM, Auroral Precipitation Model). In this work, we studied the precipitating ion behavior in the dawn (0300–0600 and 0600–0900 MLT) and dusk (1500–1800 and 1800–2100 MLT) sectors and compared their characteristics with those of electron precipitation depending on the magnetic activity level.

To distinguish the auroral precipitation regions with different characteristics, we used the generalized classification proposed in (Starkov et al., 2002). Based on the auroral particle characteristics, we distinguished three precipitation zones: diffuse auroral zone (DAZ), and auroral oval precipitation (AOP), and soft diffuse precipitation region (SDP). The DAZ is located equatorward of the auroral oval and spatially coincides with the diffuse auroral luminosity band. The AOP region is related to structured precipitation, the equatorward boundary of which statistically coincides with the auroral oval equatorward boundary. The SDP zone borders the AOP region on its poleward side.

3. ELECTRON AND ION PRECIPITATION BOUNDARIES

The high-latitude boundary of auroral precipitation is characterized by the SDP poleward boundary, the latitude of which is identical for electrons and ions during each satellite pass. Based on the precipitation characteristics, this boundary can be considered as a polar cap boundary. The equatorward boundary of DAZ (DAZ_{eq}) is the low-latitude boundary of precipitation. This boundary is determined separately for electrons and ions and is identical to the *b1e* and *b1i* boundaries according to the nomenclature presented in (Newell et al., 1996). The position of the *b1e* and *b1i* boundaries during each satellite pass was registered as the lowest latitude at which the readings of the detectors of the corresponding particles in the lowest energy channels (32 and 47 eV) are twice higher than the background level (Newell et al., 1996).

The DAZ_{eq} boundary position in the (a) dawn (0300–0600 MLT) and (b) dusk (1800–2100 MLT) sectors depending on the magnetic activity level is shown in Fig. 1. The corrected geomagnetic latitude (Φ') is plotted on the ordinate. We plotted half of the rms deviation on one or another side as vertical bars in order to simplify Fig. 1. Solid and dashed lines show the equatorward boundaries of the ion and electron precipitation, respectively. In the dawn sector (a), the equatorward boundary of the electron precipitation is located lower than the ion precipitation boundary by 3°–4°; at the same time, these boundaries in the dusk sector (b) are located at approximately the same latitudes at all magnetic activity levels. Figure 1 indicates that the boundaries generally moved toward the equator with increasing magnetic activity. During quiet periods ($AL > -300$ nT), the ion precipitation equatorward boundary is located at approximately identical latitudes during the morning and evening MLT hours. However, the ion precipitation boundary shifts equatorward much faster in the dawn sector with increasing magnetic activity. At $AL \approx -1000$ nT, the DAZ_{eq}

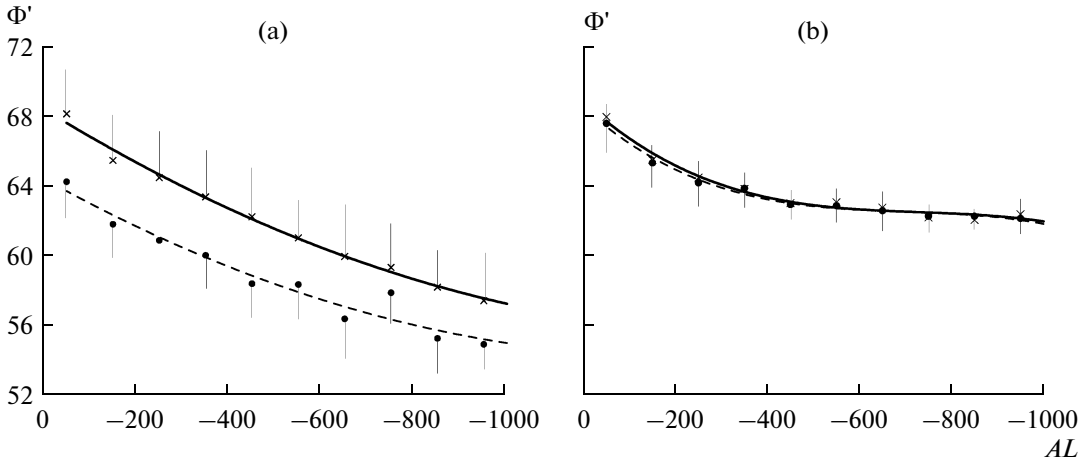

Fig. 1. The DAZ_{eq} boundary position in the (a) dawn (0300–0600 MLT) and (b) dusk (1800–2100 MLT) sectors, depending on the geomagnetic activity level. The ion and electron precipitation boundaries are shown by solid and dashed lines, respectively. Half of the rms deviation is shown with vertical bars.

boundary for ions is located at Φ' ~ 58° and Φ' ~ 62° in the dawn and dusk sectors, respectively. The position of the electron precipitation boundary differs even stronger. A dawn–dusk asymmetry in the latitudinal position of the precipitation equatorward boundary is generally observed when the magnetic activity level is high.

The DAZ poleward boundary is simultaneously the AOP equatorward boundary, statistically coincides with the auroral oval equatorward boundary, and is identified with the beginning or inner edge of the central plasma sheet in the projection on the equatorial plane of the magnetosphere (Feldstein and Galperin, 1985). This boundary is determined based on electron precipitation and corresponds to the *b2e* boundary according to the notation by (Newell et al., 1996). The latitude of the *b2i* ion precipitation boundary was determined in (Newell et al., 1996) as an isotropy boundary (Sergeev et al., 1983), which corresponds to the near-Earth edge of the current sheet in the magnetotail. According to the DMSP data, this boundary is determined based on the maximum of precipitating ion fluxes with energies higher than 3 keV.

The position of the DAZ_{pol} boundary in the (a) dawn and (b) dusk sectors depending on the *AL* index value is shown by dashed lines in Fig. 2. The solid lines in Fig. 2 show the position of the *b2i* isotropization boundary. In the dawn sector, the isotropy boundary is located a few degrees poleward of the DAZ_{pol} boundary in the AOP structured precipitation region. The latitudinal difference in the boundary position increases with increasing magnetic activity and is ~1.5° under quiet conditions and reaches ~4° when $AL = -1000$ nT. In the dusk sector, the positions of the *b2i* and DAZ_{pol} boundaries are close to each other, but the isotropy boundary is located equatorward of the DAZ_{pol} boundary in the diffuse precipitation region by ~1° at all magnetic activity levels.

In the dusk sector, the positions of the electron and ion precipitation boundaries coincide; however, the ion precipitation maximum (the *b2i* boundary) is observed in the diffuse precipitation region near the DAZ poleward edge. The latter circumstance indicates that the electron and ion flux maxima can be located at different latitudes when the boundaries coincide. We performed the following procedure in order to determine the latitudinal distribution of the precipitating particle fluxes. The coordinates of the maximal electron and ion energy fluxes in the DAZ, AOP, and SDP regions and the particle energies at these points were determined during each satellite pass. The average latitudinal distributions of such maximums in the dusk sector are illustrated by Fig. 3. The corrected geomagnetic latitude (CGL) was plotted on the abscissa in Fig. 3. Averaging was performed over each CGL degree. The distributions in Fig. 3 were constructed independently of the magnetic activity level, which was however not higher than $AL > -1000$ nT. The ion and electron precipitation characteristics are shown by solid and dashed lines, respectively. Figure 3a demonstrates that the electron (Fe) and ion (Fi) precipitation energy fluxes are separated in space. The ion and electron fluxes are maximal at latitudes of 60°–65° and 65°–74° CGL, respectively. The latitudinal energy distribution of precipitating particles is similar to the particle flux distribution, and the only difference consists in that the energy decreases much slower than the flux toward both sides of the maximal values. At all latitudes in the 1800–2100 MLT sector, the electron energy fluxes are much higher than the ion fluxes, but the ion energies are higher than the electron ones.

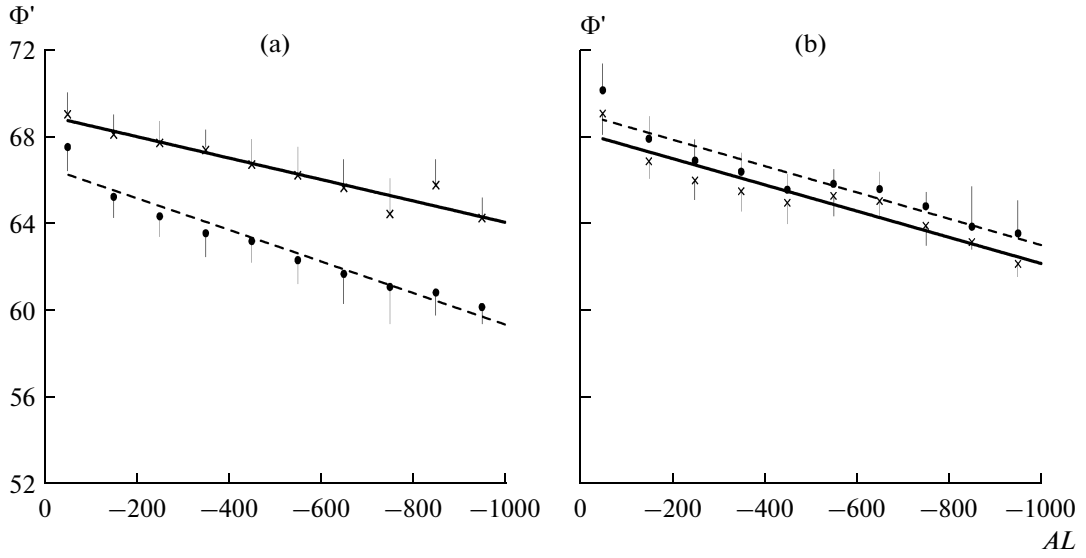

Fig. 2. Positions of the DAZ_{pol} and b2i isotropy boundaries in the (a) dawn and (b) dusk MLT sectors, depending on the *AL* index value. The *b2i* and DAZ_{pol} boundaries are shown by solid and dashed lines, respectively.

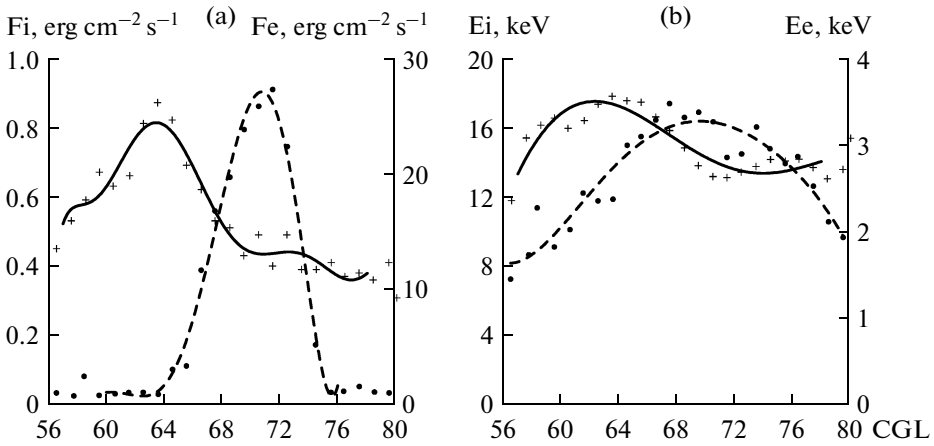

Fig. 3. Latitudinal distributions of the (a) maximal and (b) average energies of precipitating ions (solid lines) and electrons (dashed lines) in the dusk sector.

4. ION AND ELECTRON PRECIPITATION CHARACTERISTICS

The behavior of the average energy fluxes of precipitating ions (Fi) and electrons (Fe) in the (a) DAZ and (b) AOP regions depending on the magnetic activity level is shown in Fig. 4. The data were averaged in the 100-nT *AL* intervals. The experimental data were approximated by polynomials of the first and second degrees. The energy fluxes in the dawn and dusk sectors are shown by solid and dashed lines, respectively. The geomagnetic local time sectors are marked by the following numerals: (*1*) 0300–0600 MLT, (*2*) 0600–0900 MLT, (*3*) 1500–1800 MLT, and (*4*) 1800–2100 MLT.

Figure 4 indicates that the ion fluxes (the top panel) in the DAZ region (Fig. 4a) are higher in the dusk sectors than in the dawn ones, whereas the electron energies (the bottom panel) are on the contrary higher in the dawn sectors. In the 1500–1800 MLT sector (line *3*), the ion energy flux increases from approximately 0.1 to 0.3 erg cm^{-2} s^{-1} when *AL* varies from −50 to −1000 nT. In the dawn sectors, the Fi value is not larger than 0.1 erg cm^{-2} s^{-1} and is factually independent of the magnetic activity level. The electron energy fluxes are maximal in the 0300–0600 MLT sector (curve *1*) and increase from approximately 1.0 to 5.0 erg cm^{-2} s^{-1} with increasing magnetic activity. In the dusk sectors, the average electron energy fluxes are not higher than 1.0 erg cm^{-2} s^{-1} and weakly depend on the magnetic activity level.

In the AOP region of structured precipitation (Fig. 4b), the ion and electron energy fluxes decrease in going from the nightside hemisphere (curves *1*, *4*) to the day-

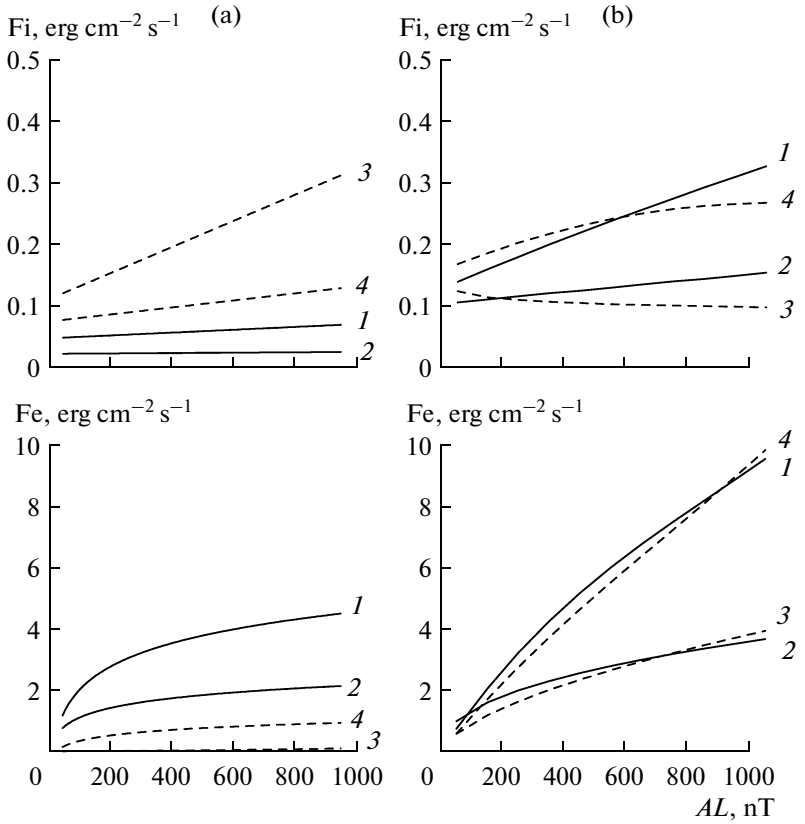

Fig. 4. Ion (Fi) and electron (Fe) energy fluxes in the (a) DAZ and (b) AOP regions, depending on the magnetic activity level. The dawn and dusk sectors are shown by solid and dashed lines, respectively: (*1*) 0300–0600 MLT, (*2*) 0600–0900 MLT, (*3*) 1500–1800 MLT, and (*4*) 1800–2100 MLT.

side one (curves *2*, *3*). This difference, which is factually absent during quiet periods, becomes more and more substantial with increasing magnetic activity. When $AL \approx -1000$ nT, the particle energy fluxes in the 0300–0600 and 1800–2100 MLT sectors are higher than in the 0600–0900 and 1800–2100 MLT sectors by a factor of approximately 3. Such a behavior of the precipitating particle fluxes is most probably caused by the circumstance that particles are accelerated and dropped into the ionosphere mostly in the nightside sector during substorms, and these processes intensify with increasing substorm intensity.

The behavior of the precipitating ion and electron energies depending on the magnetic activity level is illustrated by Fig. 5. The Fig. 5 format and denotations are the same as in Fig. 4. The character of variations in the particle energy with increasing magnetic activity and the comparative characteristics of the ion (Ei) and electron (Ee) energies in different precipitation zones and MLT sectors are similar to the particle energy flux variations presented above. In the DAZ region (Fig. 5a), the ion energy is higher in the dusk sectors than in the dawn ones, whereas the electron energy is higher in the dawn sectors. In the AOP region, the ion and electron energies decrease in going from the nighttime hours to the morning and evening ones. In the 0600–0900 and 1500–1800 MLT sectors, the average ion and electron energies are 6.0–8.8 and ~1.0 keV, respectively, at all magnetic activity levels.

The ratio (in %) of the ion and electron precipitation energy fluxes (Fi/Fe) in the dawn (the top panel) and dusk (the bottom panel) sectors is shown in Fig. 6. The Fi/Fe ratios in the AOP and DAZ regions are shown by solid and dashed lines, respectively.

In the dawn sectors, the energy introduced by ions is insignificant and decreases with increasing magnetic activity. The maximal Fi/Fe ratio (~0.2) is observed here in the 0300–0600 MLT sector in the AOP zone at very low magnetic activity. This ratio rapidly decreases to ~0.05 with increasing magnetic activity. In the DAZ region, Fi/Fe is smaller than 0.05 at all magnetic activity levels.

During the evening hours, a considerable energy contribution is observed in the DAZ in the 1500–1800 MLT. The energies of precipitating electrons and ions are approximately identical here at low magnetic activity, but the ion energy fluxes start dominating already at $AL \approx -200$ nT and are approximately three times as high as the electron ones when $AL \approx -1000$ nT. In the 1800–2100 MLT sector, the contribution of the ion energy fluxes under quiet conditions accounts for

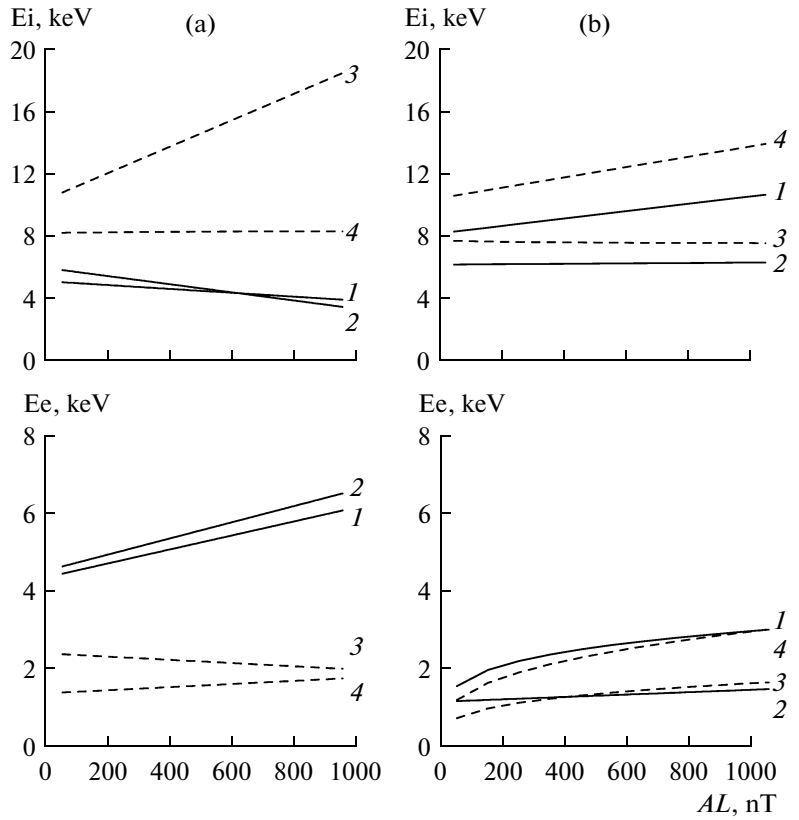

Fig. 5. Average ion (Ei) and electron (Ee) energies, depending on the magnetic activity level. The denotations are the same as in Fig. 4.

20 and 30% of the electron energy fluxes in the AOP and DAZ regions, respectively. As in the dawn sectors, the Fi/Fe ratio decreases rapidly with increasing magnetic activity.

5. DISCUSSION

To study the comparative characteristics of ion and electron precipitation in the dawn and dusk MLT sectors, we used a database created previously based on the DMSP F6 and F7 satellite observations. We thoroughly studied the precipitation characteristics depending on the magnetic activity level in the DAZ and AOP zones. We considered the characteristics of the average particle energies and energy fluxes in the 0300–0600, 0600–0900, 1500–1800, and 1800–2100 MLT sectors.

The main results of the performed studies can be formulated as follows.

1. In the dusk sector, the positions of the electron and ion precipitation boundaries approximately coincide at all magnetic activity levels; however, the latitudinal distribution of the energy fluxes indicates that the maximum positions for electrons and ions are separated in space. The ion and electron flux maxima are observed at the equatorward and poleward precipitation edges, respectively. The *b2i* isotropy boundary is located near the poleward edge of the DAZ region at all magnetic activity levels.

2. In the dawn sector, the electron precipitation region is wider than the ion precipitation region and extends to lower latitudes relative to the latter by 3°–4°. The isotropy boundary is located poleward of the DAZ_{pol} boundary in the AOP region by several degrees. The latitudinal difference in the positions of these boundaries increases with increasing magnetic activity from ~1.5° under quiet conditions to ~4° at $AL = -1000$ nT.

3. The equatorward boundaries of ion and electron precipitation shift toward the equator with increasing magnetic activity. In this case, the boundaries shift much faster in the dawn sector than in the dusk one. As a result, the dawn–dusk asymmetry in the precipitation region latitudinal position is observed at high magnetic activity.

4. Electron precipitation predominates in the dawn sector. The ion energy fluxes (Fi) account for less than 5% of the electron flux energy (Fe) in this sector in the DAZ region. In the AOP region, the contribution of Fi decreases with increasing magnetic activity from ~10–20% at $AL \approx -100$ nT to <5% at $AL \approx -1000$ nT.

5. Electron precipitation also predominates in the dusk sector of the AOP region, whereas the ion energy

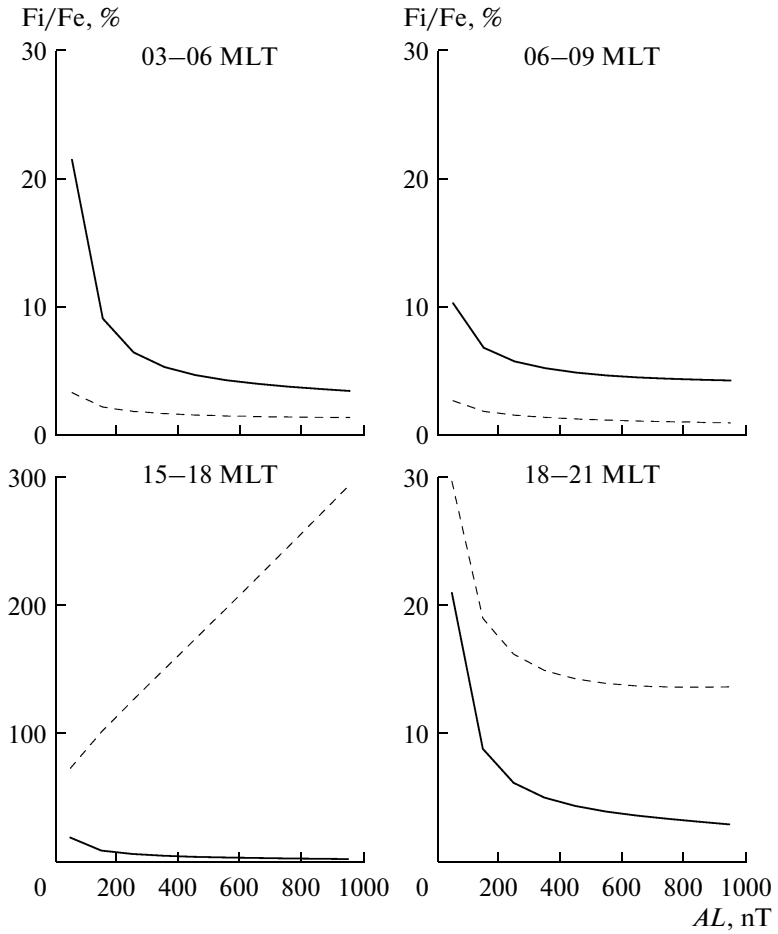

Fig. 6. Ratio of the ion and electron precipitation energy fluxes (Fi/Fe) in the dawn (the top panel) and dusk (the bottom panel) MLT sectors. The AOP and DAZ regions are shown by solid and dashed lines, respectively.

fluxes are considerable in the DAZ region. In the 1500–1800 MLT sector, the Fi/Fe ratio increases from ~0.7 to ~3.0 when *AL* varies from −100 to −1000 nT.

6. In the AOP region of structured precipitation, the ion and electron energy fluxes decrease in going from the nighttime hours to the morning and evening ones. This difference, which is factually absent during quiet periods, becomes more and more substantial with increasing magnetic activity.

The obtained data indicate that the electron precipitation region in the dawn sector is much wider than the ion precipitation region and extends to lower latitudes than the latter region. The relative position of the *b2i* and DAZ_{pol} boundaries indicates that the ion precipitation maximum in the dawn sector is located in the structured precipitation AOP region. These results qualitatively agree with the previous conclusions that the electron precipitation oval is located equatorward of the ion precipitation region (Gussenhoven et al., 1987; Hardy et al., 1989; Coumans et al., 2002). Therefore, the relative position of electron and ion precipitation in the dawn sector was not studied in more detail in the scope of this work.

The conclusion that the position of the electron and ion precipitation equatorward boundaries in the dusk sector coincides at all magnetic activity levels differs from the conclusion drawn in (Gussenhoven et al., 1987) based on an analysis of the same DMSP F6 satellite data. These authors arrived at the conclusion that the ion precipitation boundary in the evening hours is located equatorward of the electron precipitation boundary by an average of 1.4°. This difference ($\Delta\Phi$) in the position of the boundaries is not so considerable as in the dawn sector and can be questioned based on the following circumstances. Gussenhoven et al. (1987) used in their studies data for only one month (January 1983). The statistics is not too extensive; therefore, the occurrence probability distribution of different $\Delta\Phi$ values is not Gaussian but more probably Poisson with the maximum between $\Delta\Phi = 0–1°$. Second, these authors used the 3-h *Kp* index in order to determine the magnetic activity level. The time during which the satellite crosses the precipitation zone is only 2–3 min. Therefore, the level of actual magnetic activity during a satellite pass can be very widely variable at any fixed *Kp*. This will result in a considerable

spread in the position of the boundaries depending on *Kp*. No wonder that the authors used the standard deviation rather than the rms one in order to estimate the error.

Different criteria were used in the present work and in (Gussenhoven et al., 1987) in order to determine the precipitation equatorward boundary. Gussenhoven et al. (1987) determined this latitude based on a sharp increase in the total particle flux integrated over all energy channels (Gussenhoven et al., 1983). The determination of the ion boundaries was often complicated by the presence of considerable flux fluctuations. In such cases, the boundary was determined as the lowest latitude where fluctuations were registered.

In the scope of the present study, as electron and ion precipitation boundaries, we considered the *b1e* and *b1i* boundaries, the criteria for the determination of which are considered in detail in (Newell et al., 1996). We also note that these boundaries are considered as the boundaries of convection of particles with zero energy. The boundary positions only depend on the electric and magnetic field configuration and were registered as the minimal latitude at which the energy fluxes of the corresponding particles increase twice in the lowest energy channels in three successively registered spectra as compared to the three previous spectra, based on satellite data. We consider that such an approach to the determination of the precipitation equatorward boundaries is most correct.

In spite of the fact that the electron and ion precipitation boundaries in the dusk sector coincide according to our studies, the energy flux latitudinal distribution indicates that the electron and ion maximum positions are spatially separated. The ion energy fluxes are maximal equatorward of the maximal electron energy fluxes. In this respect, we can state that the ion precipitation oval is shifted equatorward of electron precipitation. This should be especially substantial according to the satellite optical observations since the N_2 LBH and Lyman-α intensity is proportional to the energy fluxes of precipitating electrons and ions, respectively.

In the dusk sector, the ion energy fluxes are maximal in the DAZ region, where they can be three times as high as the electron energy fluxes at high magnetic activity. At the same time, the ion energy fluxes are only ~0.3 erg cm^{-2} s^{-1} at $AL = -1000$ nT, which is lower than the electron fluxes in the AOP region of structured precipitation by an order of magnitude.

The fluxes of precipitating ions are maximal near the *b2i* boundary. This boundary is the isotropy boundary (Sergeev et al., 1983) and is a good proxy of the position of the near-Earth current sheet (Newell et al., 1996, 1998) in the magnetospheric tail. The DAZ_{pol} boundary statistically coincides with the auroral oval equatorward boundary and is identified with the beginning or inner edge of the central plasma sheet (CPS) in the projection on the magnetospheric equatorial plane (Feldstein and Galperin, 1985). The isotropy boundary is within CPS in the dawn sector at all magnetic activity levels and is outside this sheet at a smaller distance to the Earth than the CPS inner boundary in the dusk sector. Correspondingly, the maximal ion energy fluxes are also observed in the AOP region in the dawn sector and in the DAZ region in the dusk sector. When magnetic activity is high ($AL = -1000$ nT), the *b2i* boundary is on average located at ~64° CGL in the dawn sector and at ~62° CGL in the dusk sector. Since the isotropy boundary depends on the magnetic field topology, the dawn–dusk asymmetry in the position of this boundary and in the relative position of electron and ion precipitation indicates that the corresponding asymmetry is observed in the magnetotail magnetic field. The existence of such an asymmetry was referred to in (Newell et al., 1998). Based on an analysis of MLT variations in the isotropy boundary position, these authors found that the magnetospheric magnetic field in the dusk sector is smaller and more extensive than in the dawn sector. Such an asymmetry can be related to the effect of the current system of the partial ring current.

6. CONCLUSIONS

Based on the DMSP F6 and F7 satellite observations, we studied the comparative characteristics of ion and electron precipitation in the dawn and dusk MLT sectors. We indicated that the position of the electron and ion precipitation boundaries approximately coincides at all geomagnetic activity levels in the dusk sector; however, the latitudinal distribution of energy fluxes indicates that the electron and ion maximum positions are separated in space. The ion and electron energy fluxes are maximal at the equatorward and poleward edges of precipitation, respectively. In the dawn sector, the electron precipitation region is wider than the ion precipitation region and extends to lower latitudes by 3°–4° as compared to the latter region. The isotropy boundary is near the poleward edge of the DAZ region in the dusk sector at all magnetic activity levels and in the AOP region in the dawn sector. Since the isotropy boundary depends on the magnetic field topology, the dawn–dusk asymmetry in the position of this boundary and in the relative position of electron and ion precipitation indicates that the corresponding asymmetry is observed in the magnetotail magnetic field.

Electron precipitation predominates in the dawn sector. The ion energy fluxes (Fi) account for less than 5% of the electron energy flux (Fe) in this sector in the DAZ region. In the AOP region, the contribution of Fi decreases with increasing magnetic activity from ~10–20% at $AL \approx -100$ nT to <5% at $AL \approx -1000$ nT. In the dusk sector, electron precipitation also predominates in the AOP region, whereas the ion energy fluxes are considerable in DAZ. In the 1500–1800 MLT sector,

the Fi/Fe ratio increases from ~0.7 to ~3.0 when *AL* varies from −100 to −1000 nT.

ACKNOWLEDGMENTS

The DMSP F7 satellite data were taken from the JHU/APL webpages (http://sd-www.jhuapl.edu/); the magnetic activity indices, from IDC-A (Kyoto) (http://wdc.kugi.kyoto-u.ac.jp/).

This work was supported by the Russian Foundation for Basic Research (project no. 12-05-00273) and by the Russian Academy of Sciences (programs nos. 4 and 22).

REFERENCES

Akasofu, S.-I., Discrete, continuous and diffuse auroras, *Planet. Space. Sci.*, 1974, vol. 22, pp. 1723–1726.

Basu, B., Jasperse, J.R., Robinson, R.M., Vondrak, R.R., and Evans, D.S., Linear transport theory of auroral proton precipitation: A comparison with observations, *J. Geophys. Res.*, 1987, vol. 92, pp. 5920–5932.

Bisikalo, D.V., Shematovich, V.I., Gerard, J.-C., Meurant, M., Mende, S.B., and Frey, H.U., Remote sensing of the proton aurora characteristics from IMAGE–FUV, *Ann. Geophys.*, 2003, vol. 21, pp. 2165–2173.

Burch, J.L., Lewis, W.S., Immel, T.J., Anderson, P.C., Frey, H., Fuselier, S.A., Gerard, J.C., Mende, S.B., Mitchell, D.G., and Thomsen, M.F., Interplanetary magnetic field control of afternoon sector detached auroral arcs, *J. Geophys. Res.*, 2002, vol. 107, p. 1251. doi:10.1020/2001JA007554

Coumans, V., Gerard, J.-C., Hubert, B., and Evans, D.S., Electron and proton excitation of the FUV aurora: Simultaneous IMAGE and NOAA observations, *J. Geophys. Res.*, 2002, vol. 107A, pp. 1374–1359.

Coumans, V., Gerard, J.-C., Hubert, B., Meurant, M., and Mende, S.B., Global auroral conductance distribution due to electron and proton precipitation from IMAGE–FUV observations, *Ann. Geophys.*, 2004, vol. 22, pp. 1595–1611.

Evlashin, L.S., Hydrogen emission in auroras and auroral proton precipitation, in *Fizika okolozemnogo kosmicheskogo prostranstva* (Physics of the Near-Earth Space), Apatity, 2000, vol. 3, pp. 500–548.

Feldstein, Y.I. and Galperin, Y.I., The auroral luminosity structure in the high-latitude upper atmosphere: Its dynamics and relationship to the large-scale structure of the Earth's magnetosphere, *Rev. Geophys.*, 1985, vol. 23, pp. 217–275.

Gussenhoven, M.S., Hardy, D.A., and Heinemann, N., Systematics of the equatorward diffuse auroral boundary, *J. Geophys. Res.*, 1983, vol. 88A, pp. 5692–5708.

Gussenhoven, M.S., Hardy, D.A., and Heinemann, N., The equatorward boundary of auroral ion precipitation, *J. Geophys. Res.*, 1987, vol. 92A, pp. 3273–3283.

Hardy, D.A., Gussenhoven, M.S., and Holeman, E., A statistical model of auroral electron precipitation, *J. Geophys. Res.*, 1985, vol. 90A, pp. 4229–4248.

Hardy, D.A., Gussenhoven, M.S., and Brautigan, D., A statistic model of auroral ion precipitation, *J. Geophys. Res.*, 1989, vol. 94A, pp. 370–392.

Immel, T.J., Mende, S.B., Frey, H.U., Peticolas, L.M., Carlson, C.W., Gerard, J.C., Hubert, B., Fuselier, S., and Burch, J.L., Precipitation of auroral protons in detached arcs, *Geophys. Res. Lett.*, 2002, vol. 29. doi:10.1029/2001GL03847.

Meinel, A.B., Doppler-shifted auroral hydrogen emission, *Astrophys. J.*, 1951, vol. 113, pp. 50–61.

Newell, P.T., Feldstein, Y.I., Galperin, Y.I., and Meng, C.-I., The morphology of nightside precipitation, *J. Geophys. Res.*, 1996, vol. 101A, pp. 10 737–10 748.

Newell, P.T., Sergeev, V.A., Bikkuzina, G.R., and Wing, S., Characterizing the state of the magnetosphere: Testing the ion precipitation maxima latitude (*b2i*) and the ion isotropy boundary, *J. Geophys. Res.*, 1998, vol. 103A, pp. 4739–4745.

Reidler, W., Auroral particle precipitation pattern, in *Earth Magnetospheric Processes*, McCormac, B.M., Ed., Hingham: Reidal, 1972.

Reidler, W. and Borg, H., High latitude precipitation of low energy particles observed by ESRO 1A, *Space Res.*, 1972, vol. 12, pp. 1397–1403.

Senior, C., Sharber, J.R., de la Beaujardiere, O., Heelis, R.A., Evans, D.S., Winningham, J.D., Sugiura, M. and Hoegy, W.R., *E* and *F* region study of the evening sector auroral oval: A Chatanika Dynamics Explorer 2 NOAA 6 comparison, *J. Geophys. Res.*, 1987, vol. 92, pp. 2477–2494.

Sergeev, V.A., Sazhina, E.M., Tsyganenko, N.A., Lundblad, J.A., and Soraas, F., Pitch-angle scattering of energetic protons in the magnetotail current sheet as the dominant source of their isotropic precipitation into the nightside ionosphere, *Planet. Space Sci.*, 1983, vol. 31, no. 10, pp. 1147–1155.

Starkov, G.V., Rezhenov, B.V., Vorobjev, V.G., Feldstein, Ya.I., and Gromova, L.I., Dayside auroral precipitation structure, *Geomagn. Aeron.*, 2002, vol. 42, no. 2, pp. 176–183.

Vegard, L., Hydrogen showers in the auroral region, *Nature*, 1939, vol. 144, no. 3661, pp. 1089–1090.

Vorobjev, V.G. and Yagodkina, O.I., Effect of magnetic activity on the global distribution of auroral precipitation zones, *Geomagn. Aeron.*, 2005, vol. 45, no. 4, pp. 438–444.

Translated by Yu. Safronov